Development 140, 3254-3265 (2013) doi:10.1242/dev.094938

Pdgfra protects against ethanol-induced craniofacial defects in a zebrafish model of FASD

Neil McCarthy[1], Leah Wetherill[2], C. Ben Lovely[1], Mary E. Swartz[1], Tatiana M. Foroud[2] and Johann K. Eberhart[1,*]

SUMMARY

Human birth defects are highly variable and this phenotypic variability can be influenced by both the environment and genetics. However, the synergistic interactions between these two variables are not well understood. Fetal alcohol spectrum disorders (FASD) is the umbrella term used to describe the wide range of deleterious outcomes following prenatal alcohol exposure. Although FASD are caused by prenatal ethanol exposure, FASD are thought to be genetically modulated, although the genes regulating sensitivity to ethanol teratogenesis are largely unknown. To identify potential ethanol-sensitive genes, we tested five known craniofacial mutants for ethanol sensitivity: *cyp26b1*, *gata3*, *pdgfra*, *smad5* and *smoothened*. We found that only *platelet-derived growth factor receptor alpha* (*pdgfra*) interacted with ethanol during zebrafish craniofacial development. Analysis of the PDGF family in a human FASD genome-wide dataset links *PDGFRA* to craniofacial phenotypes in FASD, prompting a mechanistic understanding of this interaction. In zebrafish, untreated *pdgfra* mutants have cleft palate due to defective neural crest cell migration, whereas *pdgfra* heterozygotes develop normally. Ethanol-exposed *pdgfra* mutants have profound craniofacial defects that include the loss of the palatal skeleton and hypoplasia of the pharyngeal skeleton. Furthermore, ethanol treatment revealed latent haploinsufficiency, causing palatal defects in ~62% of *pdgfra* heterozygotes. Neural crest apoptosis partially underlies these ethanol-induced defects in *pdgfra* mutants, demonstrating a protective role for Pdgfra. This protective role is mediated by the PI3K/mTOR pathway. Collectively, our results suggest a model where combined genetic and environmental inhibition of PI3K/mTOR signaling leads to variability within FASD.

KEY WORDS: Zebrafish, Alcohol, Pdgfra, FAS, mTOR

INTRODUCTION

Phenotypic variability is typical in human disorders. This variability can be caused by a combination of genetic and environmental factors. Although we have gained insight into these separate genetic and environmental influences, the synergistic interactions between the two are largely unknown. We sought to understand these interactions by examining the effects of embryonic alcohol exposure on craniofacial development using a zebrafish model.

Fetal alcohol spectrum disorders (FASD) encompass the range of defects associated with prenatal exposure to ethanol. By some estimates, FASD affect somewhere from 1% of the North American population (Sampson et al., 1997) to 2-5% of the USA and Western Europe (May et al., 2005; May et al., 2007). Defects and deficits associated with FASD are variable and lie along a continuum with the most severe form represented by fetal alcohol syndrome (FAS), which is clinically diagnosed by growth retardation, deficiencies in brain growth (reduced head circumference and/or structural brain anomaly) and distinct facial features (microcephaly, short palpebral fissures, thin upper lip and/or smooth philtrum) (Jones and Smith, 1973). Other craniofacial defects can arise in FAS, including cleft palate (Swayze et al., 1997). The variability of the defects found in FAS and FASD are partly attributed to the timing and dose of fetal exposure to ethanol (Ali et al., 2011; Sulik, 2005; Sulik et al., 1986). However, genetic factors are also likely to influence FASD, yet these influences are poorly understood.

Several lines of evidence suggest a genetic component to FASD (Warren and Li, 2005). Different strains of mice, rats, chickens and zebrafish show differing sensitivity to ethanol exposure (Boehm et al., 1997; Debelak and Smith, 2000; Dlugos and Rabin, 2003; Thomas et al., 1998). Recently, work in mouse has shown that the Hedgehog (Hh) pathway gene, *Cdon*, interacts with ethanol (Hong and Krauss, 2012). The Hh pathway has also recently been shown to interact with ethanol during zebrafish neural development (Zhang et al., 2013). In humans, the most compelling evidence for a genetic component to FASD is twin studies showing greater concordance for FAS between monozygotic than for dizygotic twins (Streissguth and Dehaene, 1993). In a small South African cohort, resistance to FAS associates with carrying the alcohol dehydrogenase (ADH) B*2 allele, which catabolizes alcohol at a faster rate than other ADH isozymes (Viljoen et al., 2001). Together, these studies provide evidence for gene-environment interactions being involved in susceptibility to FASD.

The zebrafish provides an excellent model system in which to study gene-ethanol interactions. Zebrafish eggs are fertilized externally, simplifying the analysis of zygotic genes that interact with ethanol. Furthermore, this external development allows for the precise timing and dosage of ethanol exposure. Zebrafish embryos display FASD defects when exposed to ethanol and the effects of ethanol timing and dosage have been well studied in zebrafish as far back as 1910 (Ali et al., 2011; Arenzana et al., 2006; Dlugos and Rabin, 2003; Lockwood et al., 2004; Loucks and Carvan, 2004;

[1]Department of Molecular and Cell and Developmental Biology, Institute for Cellular and Molecular Biology and Institute for Neuroscience, University of Texas, Austin, TX 78712, USA. [2]Department of Medical and Molecular Genetics, Indiana University School of Medicine, Indianapolis, IN 46202, USA.

*Author for correspondence (eberhart@austin.utexas.edu)

Accepted 4 June 2013

Stockard, 1910). Yet we know very little about how genetic factors influence ethanol-induced phenotypes, such as perturbations of proper craniofacial development.

In all vertebrate species, the majority of the craniofacial skeleton derives from the cranial neural crest (Couly et al., 1993; Evans and Noden, 2006; Gross and Hanken, 2008; Knight and Schilling, 2006; Le Lievre, 1978; Noden, 1978; Yoshida et al., 2008). Neural crest cells are generated between neural and non-neural ectoderm. Neural crest cells undergo an epithelial-to-mesenchymal transition, which allows them to migrate into the periphery to form a wide variety of cell types (Theveneau and Mayor, 2012). In cranial regions, these cells will migrate into serially reiterated structures called pharyngeal arches (Grevellec and Tucker, 2010). In the zebrafish, this occurs beginning at 10 hours post-fertilization (hpf) and ends around 30 hpf (Eberhart et al., 2008). Morphogenetic processes within the pharyngeal arches will eventually shape the craniofacial skeleton by 5 days post-fertilization (dpf). In the zebrafish, the first pharyngeal arch contributes to jaw structures, including Meckel's cartilage and the palatoquadrate, as well as to palatal elements, including the ethmoid plate and trabeculae (Cubbage and Mabee, 1996; Kesteven, 1922; Shah et al., 1990; Swartz et al., 2011). The second arch contributes to the jaw support skeleton, including the hyosymplectic, ceratohyal and interhyal cartilages.

Numerous signaling pathways regulate the development of these craniofacial elements, including the platelet-derived growth factor (Pdgf) signaling pathway. Pdgfra is a receptor tyrosine kinase, known to regulate a number of processes, including cellular migration, proliferation and survival (Tallquist and Kazlauskas, 2004; Wu et al., 2008). A key effector of Pdgfra signaling is PI3K, which can regulate numerous cell behaviors, including migration via activation of small GTPases and survival and growth via activation of mTOR (Downward, 2004; Klinghoffer et al., 2002; Zhou and Huang, 2010). In both mouse and zebrafish, most, if not all, cranial neural-crest cells express Pdgfra and Pdgfra function is required in the neural crest (Eberhart et al., 2008; Soriano, 1997; Tallquist and Soriano, 2003). Although the precise function of Pdgfra is not known in mouse, in zebrafish Pdgfra is necessary for proper neural crest cell migration (Eberhart et al., 2008).

The work described here uncovers a second role for *pdgfra* in the neural crest: protection against ethanol-induced teratogenesis. Testing five craniofacial mutants, *cyp26b1*, *gata3*, *pdgfra*, *smad5* and *smoothened*, for dominant enhancement of ethanol teratogenesis, we found that only *pdgfra* heterozygotes and mutants showed enhanced craniofacial defects after ethanol exposure. In a small human dataset with variable prenatal alcohol exposure, we find support for a gene-ethanol interaction with single nucleotide polymorphisms (SNPs) in PDGF family members that associate with different craniofacial phenotypes. In zebrafish, the susceptibility to craniofacial defects is at least partly due to neural crest cell apoptosis following ethanol exposure. The *pdgfra*-ethanol interaction is due to the combined genetic and environmental attenuation at or downstream of the mechanistic target of rapamycin (mTOR), part of the phosphoinositide 3 kinase (PI3K) pathway. Collectively, our data show that genetic screens using zebrafish will have important implications in FASD research, both in uncovering genetic susceptibility loci and in characterizing the mechanisms underlying gene-ethanol interactions.

MATERIALS AND METHODS

Danio rerio (zebrafish) care and use

All embryos were raised and cared for using established protocols (Westerfield, 1993) with IACUC approval from the University of Texas at Austin. *Tg(fli1:EGFP)y1* transgenic embryos (Lawson and Weinstein, 2002) are called *fli1:EGFP* throughout the text. Embryos were treated in embryo media with 1.0% and 0.5% ethanol, 1.5 µM wortmannin (W1628, Sigma), 3 µM rapamycin (S1120, Selleck) and 25 µM caspase inhibitor 3 (Cat#264155, Calbiochem). L-leucine has been used at 100 mM in zebrafish (Payne et al., 2012), but we found that a 50 mM solution was sufficient to provide rescue in our experiments. The *pdgfra*^{b1059} (Eberhart et al., 2008), *smad5*^{b1100} (Sheehan-Rooney et al., 2013) and *smo*^{b577} (Varga et al., 2001) alleles have been described previously. The *gata3*^{b1075} and *cyp26b1*^{b1024} alleles were recovered from a forward genetic screen at the University of Oregon. To determine ethanol tissue concentration relative to media exposure, headspace gas chromatography (GC) was used (C.B.L., Rueben A. Gonzales and J.K.E., unpublished).

Morpholino and RNA injection

Approximately 3 nl of morpholinos (Gene Tools), working concentrations 3.5 mg/ml *ptena*/*ptenb* (Croushore et al., 2005), and 1.2 mM *mir140* (Eberhart et al., 2008), were injected into one- or two-cell stage zebrafish embryos. *pdgfra* mRNA was made as described previously (Eberhart et al., 2008).

Immunohistochemistry

Embryos were fixed and prepared for immunohistochemistry following the procedure outlined previously (Maves et al., 2002) using anti-active caspase 3 (Promega) and phospho-Histone H3 (Sigma) primary antibodies with Alexa Fluor 568 anti-rabbit IgG (Invitrogen) secondary antibodies. For quantification of the ratio of cell death, embryos were counterstained with ToPro (Invitrogen) and all nuclei within a single representative *z* plane were aligned through the lateral 1st and 2nd arches, such that the oral ectoderm and 1st pouch, but not the mesodermal cores, were visible.

Immunoblotting

Mutants were visually sorted from wild-type/heterozygotes by their neural crest cell migration defect (Eberhart et al., 2008). Embryos were euthanized, dechorionated and then de-yolked using a fire-pulled glass pipette. Heads were separated from the tail at the posterior end of the otic vesicle. Immunoblotting was performed as described (Tittle et al., 2011) using primary antibodies AKT, pAKT, eIF4B, peIF4B and b-actin (all from Cell Signaling), and anti-rabbit secondary antibody (Cell Signaling). Membranes were reprobed using stripping buffer containing 0.2 M glycine, 0.05% Tween-20 (pH 2.5) for 30 minutes at 70°C. Membranes were washed twice with TBST, reblocked for 1 hour at room temperature and placed in primary antibody. ImageJ was used to quantify blots (Schneider et al., 2012).

Cartilage and bone staining and area measurements

Five day postfertilization (dpf) zebrafish embryos were stained with Alcian Blue and Alizarin Red (Walker and Kimmel, 2007), then flat mounted (Kimmel et al., 1998). Images were taken with a Zeiss Axio Imager-AI microscope, and palate and neurocranial lengths and widths and jaw and jaw-support elements were measured using AxiovisionLE software (AxioVs40 V4.7.1.0). All graphs were made in Microsoft Excel 2011. We used ANOVA followed by a Tukey-Kramer post-hoc test for all statistical analyses.

Confocal microscopy and figure processing

Confocal *z*-stacks were collected on a Zeiss LSM 710 using Zen software. Images were processed in Adobe Photoshop CS.

Statistical analysis

Origin 7.0 was used for one-way ANOVA and Tukey's range test for the cell death, cell death ratio, palate and neurocranial, and pharyngeal arch measurement analysis, statistical significance was set at 0.05. Graphpad Prism 5.02 was used for the gas chromatography data.

Human samples

The published data were collected as part of an ongoing international consortium, the Collaborative Initiative on Fetal Alcohol Spectrum Disorders (CIFASD). Participants were recruited from three sites (San Diego and Los Angeles, CA, and Atlanta, GA, USA). This study was approved by the Institutional Review Board at each site. All participants and/or their parent(s)/legal guardian(s) provided written informed consent.

As part of the study visit, each participant was examined by a trained dysmorphologist who completed a standardized, uniform assessment (Jones et al., 2006). Individuals with a recognizable craniofacial syndrome other than FAS were excluded. An objective classification system, based solely on structural features (palpebral fissure, philtrum and vermillion border) and growth deficiency (head size and height and/or weight) consistent with the revised Institute of Medicine criteria (Hoyme et al., 2005), was used to classify subjects. Under this scheme, a participant could receive a preliminary diagnosis of FAS, no FAS, or deferred (Jones et al., 2006). Alcohol exposure data were collected at the interview or from a review of available study data. The extent of reported prenatal alcohol exposure information was then classified into one of three categories: none, minimal (>1 drink/week average and never more than two drinks on any one occasion during pregnancy) and greater than minimal (>4 drinks/occasion at least once/week or >3 drinks/week). Alcohol exposure was confirmed via review of records or maternal report, if available (Mattson et al., 2010).

As part of the study visit, a three-dimensional facial image was collected using the 3dMD system (3dMD, Atlanta, Georgia). Landmarks were identified on the 3D model and used to obtain linear measurements. Replication of landmark placement was required, with less than 2 mm difference per linear measurement. If the tolerance criterion was not met, a third measurement was taken and the average of the two closest measurements was chosen for analysis. For bilateral measurements, only the left side was used in analyses. Although a set of 16 standard anthropometric measurements (Moore et al., 2007) were obtained, for this study we only used a subset: inner canthal width, outer canthal width, lower facial height, lower facial depth and midfacial depth – which best modeled the craniofacial defects seen in the zebrafish model.

Genomewide single nucleotide polymorphism (SNP) genotyping was completed at the Johns Hopkins GRCF SNP Center using OmniExpress genome array, which includes over 700,000 SNPs. Standard review of both sample and SNP was performed. Race and ethnicity were reported by the participant or the parent/guardian as part of the study visit and were then confirmed based on the SNP genotypes using a principal component analysis. To reduce phenotypic heterogeneity due to race, we limited the analyses to those subjects who, based on their SNP genotypes, were of European-American descent (n=102).

The regulation and function of PDGF signaling is highly conserved across vertebrate species; therefore, we identified the SNPs within each of the five genes in the PDGF pathway. Owing to the small size of *PDGFA* (12,700 bp), no SNPs were genotyped or analyzed in this gene; therefore, we could only test the role of five out of the six genes in the PDFG pathway. Univariate analysis was performed for each SNP using linear regression framework to test whether the SNP genotype × alcohol exposure interaction accounted for a significant proportion of the variation in the five key anthropometric measures. Within the model, we also included the main effects of SNP genotype and alcohol exposure. All measures were corrected for age and gender. We used a Bonferroni correction for the number of genes (five genes) being tested, which resulted in a significance threshold of 0.01 (0.05/5).

Ethics statement

Institutional Review Board approval was obtained at each site. All participants and/or their parent(s)/legal guardian(s) provided written informed consent. All zebrafish embryos were raised and cared for using established protocols with IACUC approval (Westerfield, 1993).

Human GWAS

The human dataset is from an ongoing international consortium, the Collaborative Initiative on Fetal Alcohol Spectrum Disorders, and has been described previously (Moore et al., 2007) (supplementary material Table S2). Genotyping was performed at the Center for Inherited Disease Research (CIDR). All DNA sources consisted of saliva samples. A total of 731,442 SNPs were genotyped on the OmniExpress array, of which 728,140 SNPs passed CIDR genotyping control and were released for analysis. Out of the 240 samples submitted for genotyping, three samples were dropped by CIDR due to poor quality genotyping. Two additional samples were dropped due to chromosomal abnormalities. All remaining individuals were genotyped on at least 98% of the SNPs. All samples were examined for cryptic relatedness and population stratification. There were 16 half-sibling pairs and 37 full sibling pairs in the sample. A principal component-based analysis was performed in eigenstrat (Price et al., 2006) on both the sample data and HapMap reference samples to assign subjects to racial groups. The final European American sample consisted of 102 individuals, of which 102 had both a 3D image and alcohol exposure information.

SNPs were included for analysis if the call rate was greater than 98% in the entire sample, and SNPs were removed if the minor allele frequency was less than 0.01 or if there was significant deviation from Hardy-Weinberg equilibrium ($P<10^{-6}$). The final dataset consisted of 688,359, of which 118 were analyzed in the PDGF pathway.

All SNPs analyzed are in supplementary material Table S2.

RESULTS

pdgfra and ethanol synergistically interact

We sought to identify gene-ethanol interactions that might underlie the craniofacial variability observed in FASD. We reasoned that some genetic loci that influence ethanol teratogenicity would cause craniofacial phenotypes when mutated. We initially screened five craniofacial mutants for ethanol sensitivity: *smo*^{b577}, *cyp26b1*^{b1024}, *gata3*^{b1075}, *smad5*^{b1100} and *pdgfra*^{b1059}. For this initial screen, embryos were placed in media containing 1% ethanol from 6 hours post-fertilization (hpf) until 5 dpf, when craniofacial phenotypes were examined. At this concentration, the tissue levels of ethanol are ~41 mM (188.6 mg/dl or 0.18 BAC), as determined by headspace gas chromatography, and wild-type embryos are largely unaffected. This is a concentration of ethanol achieved in binge drinkers (Lange and Voas, 2000). Ethanol appeared to interact only with the hypomorphic *pdgfra*^{b1059} allele, dramatically exacerbating mutant phenotypes and uncovering latent haploinsufficiency (Figs 1 and 2, discussed in greater detail below), suggesting a synergistic interaction. We partially rescued these ethanol-induced defects by *pdgfra* mRNA injection or by morpholino knockdown of *miR140*, which negatively regulates *pdgfra* (Fig. 3; supplementary material Fig. S1) (Eberhart et al., 2008), demonstrating specificity of the interaction. The variability that we observed in these rescues was consistent with the variation that we previously observed in rescuing untreated *pdgfra* mutants and our finding that the craniofacial skeleton is highly sensitive to the overall levels of Pdgfra (Eberhart et al., 2008). There are also likely to be between embryo differences in signal strength downstream of the receptor, such as altered Pten function, which would impact negative feedback into the signaling pathway (Carracedo and Pandolfi, 2008) to add to the inherent variability in these rescue experiments. Collectively, these results show that ethanol interacts with a subset of gene products involved in craniofacial development.

Untreated *pdgfra* mutants have a loss of the ethmoid plate, which leads to a significant reduction in the length of the palate (Fig. 1C, asterisk; supplementary material Fig. S2) and have slightly smaller pharyngeal skeletal elements (Fig. 2C,G-I; supplementary material Table S1). Untreated heterozygous siblings develop normally (Fig. 1B; Fig. 2B,G-I; supplementary material Fig. S2; Table S1). Treatment with 1% ethanol from 10 hpf to 5 dpf had a minor effect on the neurocranium of wild-type embryos, with 11% of treated wild types having a reduced ethmoid plate (Fig. 1D,G) and the overall length of the palate was not significantly reduced (supplementary material Fig. S2). Treated wild-type embryos displayed a slightly smaller hyosymplectic (Fig. 2I; supplementary material Table S1) cartilage; however, Meckel's cartilage and the palatoquadrate appeared unaffected (Fig. 2G,H; supplementary material Table S1). Statistical analyses of the size of these elements showed that, indeed, only the hyosymplectic was reduced by ethanol.

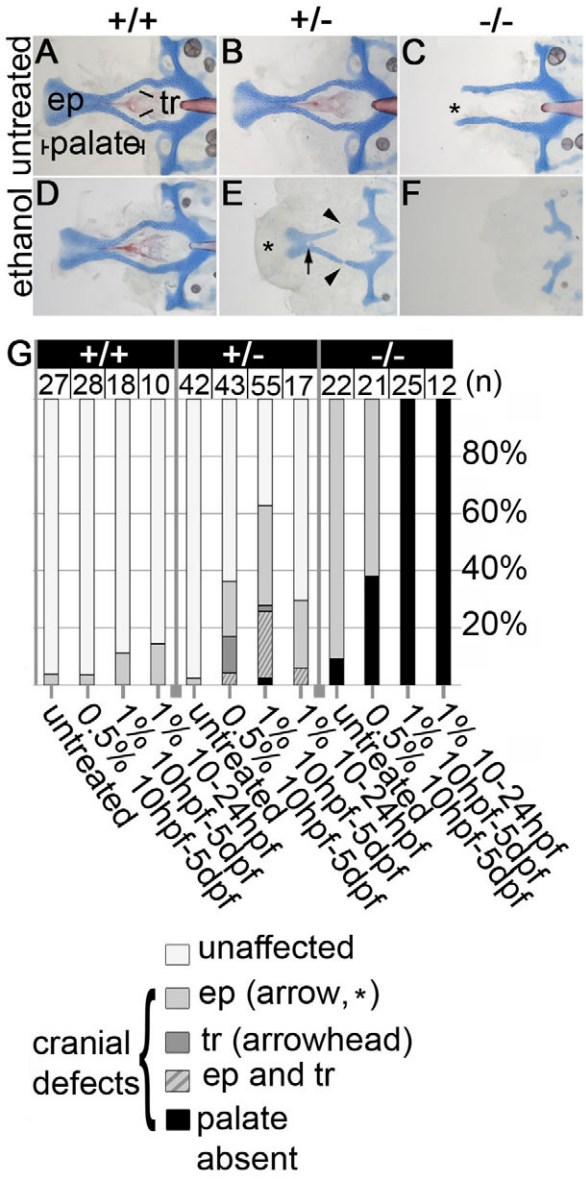

Fig. 1. Ethanol exacerbates *pdgfra* mutant neurocranial defects and reveals haploinsufficiency. (A-F) Flat-mounted 5 dpf zebrafish neurocrania. Anterior is towards the left. (**A**,**B**) Untreated wild types and *pdgfra* heterozygotes develop normally. (**C**) Untreated *pdgfra* mutants have clefting of the ethmoid plate (asterisk), although the trabeculae are typically present. (**D**,**E**) Neurocrania of embryos treated with 1.0% ethanol from 10 hours post-fertilization (hpf) to 5 days post-fertilization (dpf). (D) Wild-type embryos are predominantly normal following ethanol treatment. (E) Ethanol-treated *pdgfra* heterozygotes display variable palatal defects, including partial clefting of the ethmoid plate (asterisk), holes in the ethmoid plate (arrow) and breaks in the trabeculae (arrowheads). (**F**) Ethanol-exposed mutants have an invariant and complete loss of the palatal skeleton. (**G**) Quantification of palatal defects across genotypes and treatments. ep, ethmoid plate; tr, trabeculae.

Ethanol-treatment caused craniofacial defects in 62% of *pdgfra* heterozygotes (Fig. 1E,G), a dramatic increase compared with 11% of wild-type embryos with an identical treatment. Because heterozygous embryos rarely have craniofacial defects, this substantial increase in the number of embryos with craniofacial defects is specific to the *pdgfra*/ethanol interaction. The defects observed included gaps in the ethmoid-plate (asterisk and arrow in Fig. 1E) and breaks in the trabeculae (arrowheads in Fig. 1E). Ethanol-treated heterozygotes also displayed significantly shorter palates when compared with untreated heterozygotes and ethanol-treated wild types (supplementary material Fig. S2A). Heterozygosity for *pdgfra* alone had no effect on the size of the palatal skeleton and ethanol caused a slight, nonsignificant, reduction to the palate in wild-type siblings (supplementary material Fig. S2A). The palatal skeleton was significantly reduced in ethanol-treated *pdgfra* heterozygotes, compared with these two comparison groups. Therefore, ethanol has a specific synergistic effect on palatal development in *pdgfra* heterozygotes. Furthermore, ethanol caused a statistically significant reduction in the size of the hyosymplectic cartilage in heterozygotes compared with ethanol-treated wild types and untreated heterozygotes (Fig. 2E,I; supplementary material Table S1). Because the hyosymplectic is reduced in ethanol treated wild-type embryos and untreated heterozygotes, this effect appears additive. These results show that *pdgfra* and ethanol interact synergistically in palatal development and that the hyosymplectic is further reduced in ethanol-treated *pdgfra* heterozygotes when compared with treated wild-type embryos.

In 100% of treated *pdgfra* mutants, compared with ~10% of untreated mutants, the anterior neurocranium was completely lost (Fig. 1F). Not surprisingly, this loss led to a statistically significant decrease in the length of the palate, relative to treated wild-type embryos and untreated mutants (supplementary material Fig. S2). The ethanol-treated mutant embryos also had a statistically significant reduction of the palatoquadrate, Meckel's cartilage and the hyosymplectic compared with untreated mutant and ethanol-treated wild types and heterozygotes (Fig. 2F,G-I; supplementary material Table S1). All of the reductions observed in the ethanol-treated mutants are far beyond that predicted by an additive effect of ethanol-treatment in wild types and loss of *pdgfra* without ethanol. Ectodermal and cardiac edema was also present in 100% of treated *pdgfra* mutants (not shown). Collectively, these results provide strong support that *pdgfra* and ethanol synergistically interact during craniofacial development.

The severity and variability of ethanol-induced defects is partly dependent on concentration and developmental timing (Ali et al., 2011; Sulik, 2005). Therefore, we tested these variables across ethanol-treated *pdgfra* genotypes. We initially tested 24-hour time windows for sensitivity and then narrowed down the sensitive window. Although treatments initiating after 24 hpf had no effect, we found that a 1% ethanol treatment from 10-24 hpf is the shortest time window sufficient to fully recapitulate the mutant phenotypes obtained by treatment from 10 hpf to 5 dpf (Fig. 1G; Fig. 2G-I; supplementary material Fig. S2; Table S1). In heterozgyotes, this shorter exposure still lead to significant differences in the neurocranium, in fact the difference in length between the treated wild-type and heterozygous embryos was even more marked (Fig. 1G; supplementary material Fig. S2). No significant alterations to the hyosymplectic were observed (Fig. 2G-I; supplementary material Table S1). These results suggest that the palatal skeleton is most sensitive to brief ethanol exposure.

We tested lower ethanol concentrations to determine how sensitive *pdgfra* mutants and heterozygotes were to ethanol teratogenesis. Treatment with 0.5% ethanol, a tissue concentration of 19 mM (88 mg/dl), from 10 hpf to 5 dpf caused neurocranial defects in 3% and 13% of wild types and heterozygotes, respectively (Fig. 1G). Under these conditions, 38% of *pdgfra* mutants completely lacked the palatal skeleton (Fig. 1G). This clear increase in the percentage of heterozygous and mutant embryos with palatal

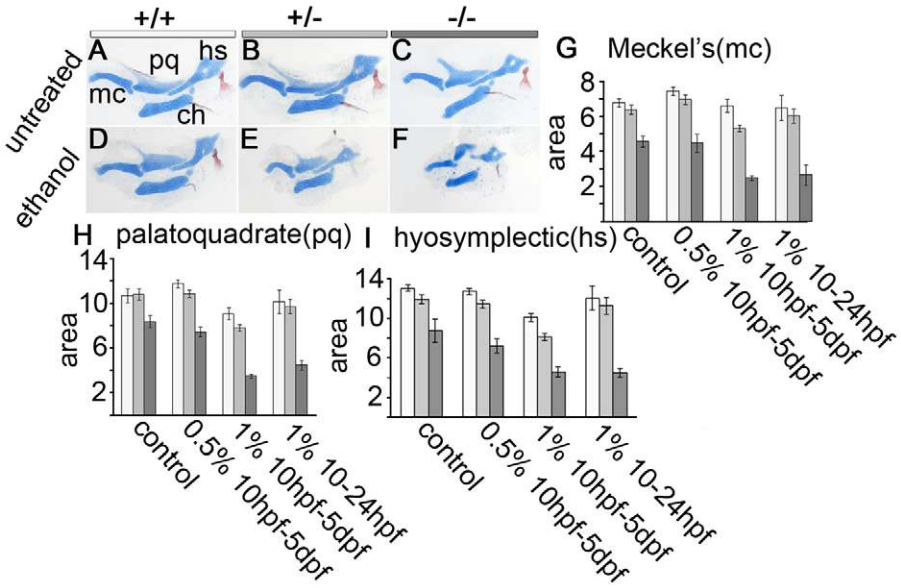

Fig. 2. Ethanol induces pharyngeal hypoplasia in *pdgfra* mutants. (**A-C**) Flat-mounted jaw and jaw support elements, anterior towards the left. Untreated (A) wild-type, (B) *pdgfra*$^{+/-}$ and (C) *pdgfra*$^{-/-}$ embryos have normally shaped cartilages. (**D**,**E**) Treatment with 1.0% ethanol from 10 hpf to 5 dpf does not affect the overall shape of cartilages in (D) wild-type or (E) *pdgfra* heterozygous embryos. (**F**) Ethanol treatment greatly disrupts the shape of the palatoquadrate and hyosymplectic cartilages in *pdgfra* mutants. (**G-I**) Quantification of the average area, in thousands of μm^2 of (G) Meckel's (mc), (H) palatoquadrate (pq) and (I) hyosymplectic (hs) cartilages (standard error bars are depicted at 1.5 s.e.m., significance is indicated by non-overlapping bars; Moses, 1987). Wild type, light bar; *pdgfra* heterozygote, light-gray bar; *pdgfra* mutants, dark-gray bar. ch, ceratohyal. Group numbers are the same as for Fig. 1.

defects is associated with reductions in the size of the crest-derived cartilages (Fig. 2G-I; supplementary material Table S1), although these differences did not reach a level of significance. Shorter treatments with 0.5% ethanol had no apparent effect (data not shown). Thus, attenuation of Pdgf signaling sensitizes embryos to ethanol-induced craniofacial defects, and this sensitivity occurs roughly when neural crest cells are migrating to and populating the pharyngeal arches, although migration does continue after 24 hpf in zebrafish palatal development (Dougherty et al., 2013).

We analyzed non-crest-derived cartilages to determine whether ethanol had a general effect on cartilage development. First, we examined the posterior neurocranium because it is of presumed mesoderm origin. Surprisingly, we discovered a previously undescribed function of Pdgfra in posterior neurocranial development, with the size of the posterior neurocranium significantly reduced in untreated mutants, relative to wild-type embryos (supplementary material Fig. S2). This requirement may relate to the requirement for Pdgfra function for migration and survival of early mesoderm precursors (Van Stry et al., 2005; Van Stry et al., 2004). As then would be expected, ethanol did interact with *pdgfra* in the development of these cartilages (supplementary material Fig. S2) to generate an overall effect of microcephaly. Second, we analyzed cartilage of the pectoral fin and found no difference between ethanol-treated mutants, ethanol-treated wild-type embryos and untreated mutants (supplementary material Fig. S3). This result suggests that there is no generalized chondrogenic defect in the ethanol-treated *pdgfra* mutants. Consistent with this, we found that *colIIa* was expressed appropriately in the posterior neurocranium of ethanol-treated mutants, although, as expected from the phenotype, no ethmoid plate or trabeculae condensations were present (supplementary material Fig. S4). Collectively, these findings show that proper development of the entire neurocranium requires Pdgfra function and that ethanol interacts synergistically, with *pdgfra* having the most profound effects on the neural crest-derived skeleton, on which we focus.

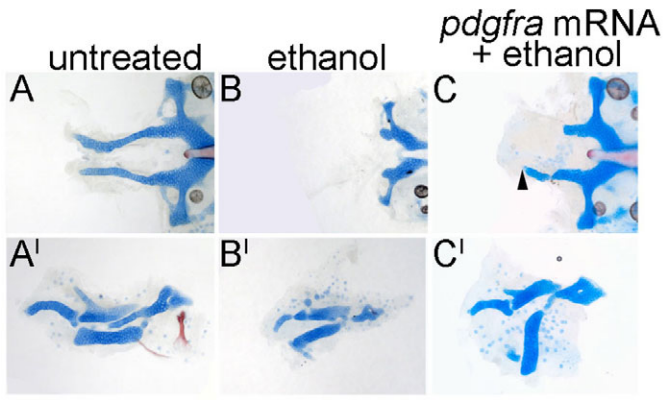

Fig. 3. *pdgfra* mRNA partially rescues the ethanol-induced defects. (**A-C**) *pdgfra* mutant 5 dpf neurocrania. (**A′-C′**) Corresponding jaw and jaw support elements. Anterior is towards the left. (A,A′) Untreated *pdgfra* mutants typically have trabeculae (*n*=13/14). (B,B′) Ethanol treatment from 10-24 hpf causes trabeculae loss in all *pdgfra* mutants (*n*=10/10). (C,C′) *pdgfra* mRNA injection partially rescues the trabeculae (C, arrowhead, *n*=3/6), and the jaw and jaw support defects in 1.0% ethanol-treated *pdgfra* mutants (note the shape of the cartilage elements in C′).

The regulation and function of Pdgf signaling is highly conserved across vertebrate species, prompting us to seek evidence from a published human sample (Jones et al., 2006) for interactions between PDGF family members and prenatal ethanol exposure. We asked whether there was evidence for ethanol use/SNP interaction on human craniofacial features. We tested members of the human PDGF family, including *PDGFB*, *PDGFC*, *PDGFD*, *PDGFRA* and *PDGFRB*, using a well-characterized sample from the USA (see supplementary material Table S2 for a complete list of the SNPs analyzed) (Mattson et al., 2010; Moore et al., 2007). Owing to the small size of *PDGFA* (12,700 bp), no SNPs were genotyped or analyzed in this gene. The best evidence for gene-ethanol interactions in humans was found in the two PDGF receptor genes. The most significant evidence for a gene-ethanol interaction was observed with two SNPs in *PDGFRB*, when analyzing midfacial depth (rs2304061, $P=3.7\times10^{-6}$; rs1075846, $P<3.5\times10^{-5}$). These SNPs are in modest linkage disequilibrium ($r^2=0.57$) and were also moderately associated with lower facial depth (both $P<9.9\times10^{-4}$). In addition, a single SNP in *PDGFRA* was associated with the measures of outer canthal width and midfacial depth ($P=1.3\times10^{-4}$ and $P=1.7\times10^{-4}$). Together, these results provide evidence that zebrafish gene-ethanol interactions may be conserved in humans.

Neural crest cell apoptosis increases in ethanol-exposed pdgfra mutants

High doses of ethanol can cause neural crest cell apoptosis (Cartwright and Smith, 1995; Sulik, 2005) and Pdgf signaling has been implicated in mesoderm-cell survival (Van Stry et al., 2005). We postulated that the craniofacial defects in ethanol-treated mutants and heterozygotes could be due, at least in part, to an increase in cranial neural crest cell death. In support of this model, treating *pdgfra* mutants with ethanol and caspase-inhibitor III partially rescued the ethanol-induced craniofacial defects (Fig. 4G, compare with Fig. 1C,F). We do not expect a full rescue with this treatment, because clefting of the ethmoid plate is due to a migratory defect (Eberhart et al., 2008). Thus, this partial rescue supports the model in which elevated apoptosis underlies some of the effect of ethanol on *pdgfra* mutants.

We directly determined the levels of apoptosis using anti-active caspase immunohistochemistry in the neural crest cell labeling *fli1:EGFP* transgenic line. We quantified neural crest cell death in the first and second arch at 20 and 24 hpf, encompassing the developmental time window in which *pdgfra* mutants are most sensitive to ethanol (Fig. 4A-D′). We did not observe any increase in cell death in ethanol-treated groups at 20 hpf compared with untreated controls (not shown). At 24 hpf, there were low levels of neural crest cell death in all untreated genotypes, ranging from one to two cells per side of the embryo (Fig. 4E). The frequency of cell death was slightly increased in ethanol-treated wild-type embryos (3.4 cells/side) and was further increased in ethanol-treated heterozygotes (4.79 cells/side, Fig. 4E), although this effect was not clearly synergistic. In ethanol-treated *pdgfra* mutants, we found a statistically significant and non-additive increase in apoptosis compared with all other groups (Fig. 4E, 10.3 cells/side, Tukey test $*P \leq 0.01$). In all ethanol-treated genotypes, there were frequently non-*fli1:GFP*-positive cells undergoing apoptosis just dorsal to the first arch, in the relative position of the trigeminal ganglion. There were, however, no global elevations in apoptosis at 24 hpf between ethanol-treated mutants and sibling counterparts compared with their untreated mutants and siblings (supplementary material Fig. S5), suggesting that the *pdgfra*-ethanol interaction leads to an increase in neural-crest specific cell death. Quantification of the ratio of cell death compared with total cells showed a linear increase in all ethanol-treated groups at 24 hpf (Fig. 4F). Ethanol treatment did not reduce cell proliferation at 24 hpf in *pdgfra* mutants relative to untreated controls; however, we did observe a rise in cell proliferation in wild-type embryos (supplementary material Fig. S6; $n=5$ for each group). This rise in proliferation may compensate for the slight increase of cell death at this time.

Although *pdgfra* mutants are most sensitive to ethanol from 10-24 hpf, the effects of ethanol could potentially continue after the treatment. Therefore, we analyzed cell death after a 6-hour recovery period from ethanol. Strikingly, we observed a significant and synergistic increase in cell death at 30 hpf, after ethanol was removed at 24 hpf in *pdgfra* mutants (14.2 cells/side, Tukey test $*P \leq 0.01$, Fig. 4E). The trend for elevated cell death in *pdgfra* heterozygotes, seen at 24 hpf, was abolished with just 6 hours recovery (Fig. 4E,F). This timing of 24-30 hpf correlates with when Pdgfra ligands begin to be expressed in the epithelia adjacent to the neural crest (Eberhart et al., 2008). These data suggest that *pdgfra* protects against ethanol-induced neural crest cell death during neural crest condensation in the arches, and may be a compensatory mechanism against ethanol-induced cell death following ethanol exposure.

Detailed fate maps of the pharyngeal arches in the zebrafish at 24 hpf allow us to compare directly the location of cell death to the skeletal structures disrupted across ethanol-treated *pdgfra* genotypes. At 24 hpf, neural-crest cells condensing on the roof of the oral ectoderm contribute to most of the anterior neurocranium (Crump et al., 2006; Eberhart et al., 2006). In addition, cells located

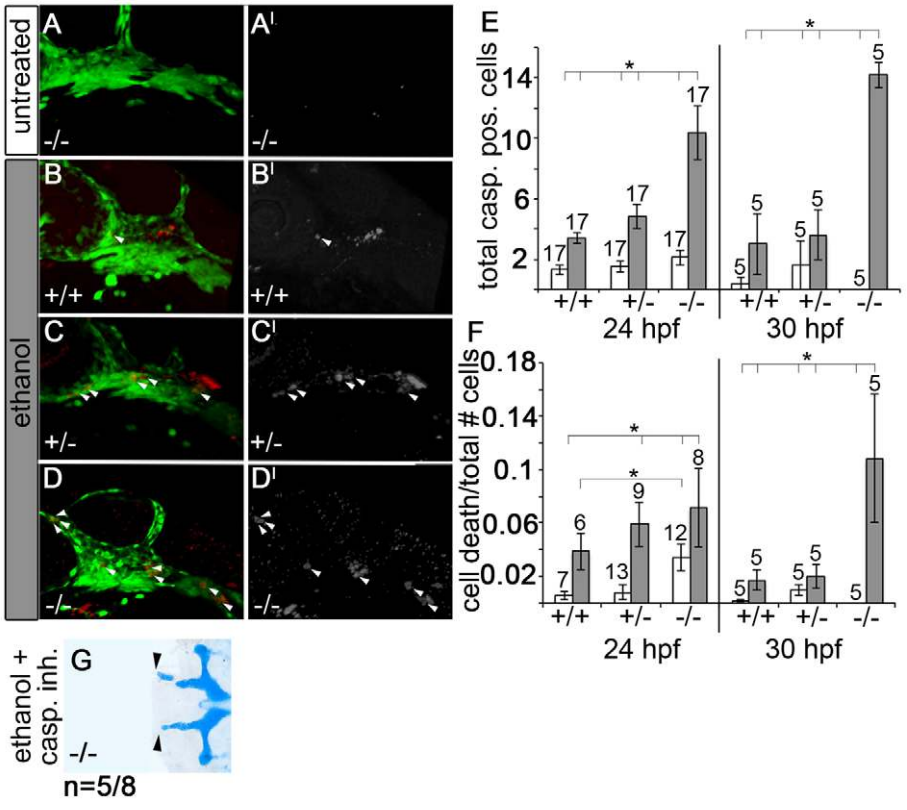

Fig. 4. Ethanol-treated *pdgfra* mutants exhibit an increase in neural crest cell death. (**A-D**) Confocal images of 24 hpf anti-active caspase 3-stained *fli1;EGFP* embryos. (**A′-D′**) Active-caspase 3 staining alone. Anterior is towards the left. (A-C′) Untreated *pdgfra* mutants, ethanol-treated wild types and ethanol-treated heterozygotes have low levels of neural crest apoptosis. (D,D′) Ethanol-treated *pdgfra* mutants have greatly elevated levels of neural crest apoptosis. Arrowheads indicate apoptotic neural crest cells. (**E**) Quantification of cell death across genotypes at 24 hpf and 30 hpf, after ethanol was removed at 24 hpf (untreated control, light bars; ethanol, dark bars). Ethanol-treated *pdgfra* mutants show significant elevation in cell death compared with all other genotypes (one-way ANOVA, $*P \leq 0.05$). (**F**) Quantification of the ratio of cell death relative to total crest cells (untreated control, light bars; ethanol, dark bars; black bars above cell death ratio indicate significant differences using one-way ANOVA, $*P \leq 0.05$). (**G**) 5 dpf *pdgfra* mutant treated with 1.0% ethanol and 25 μM caspase inhibitor at 10-24 hpf. Arrowheads indicate partial rescue of the trabeculae (compare G with Fig. 1C,F). Group numbers are indicated above the bars in each graph.

dorsally in the 1st and 2nd pharyngeal arches contribute to the palatoquadrate and hyosymplectic (Crump et al., 2004; Crump et al., 2006; Eberhart et al., 2006). These are the skeletal elements that were reduced to the greatest extent in ethanol-treated *pdgfra* mutants, and increased cell death in ethanol-treated mutants and heterozygotes occurred in these precursor regions (supplementary material Fig. S7). The regions of enhanced cell death are also adjacent to the oral ectoderm and pharyngeal pouches, sources of ligands for Pdgfra (Eberhart et al., 2008). Collectively, these data show that the *pdgfra*-ethanol interaction causes an increase in neural crest cell death starting at 24 hpf, which contributes to the ethanol-induced craniofacial defects at 5 dpf.

Combined loss of Pdgf signaling and ethanol exposure impinges on mTOR signaling

In combination with our previous analyses (Eberhart et al., 2008), our results show that Pdgf signaling functions in both neural crest migration and protection from ethanol-induced apoptosis. A main *pdgfra* effector regulating cell survival and migration *in vitro* and in *Xenopus* mesoderm cells is phosphoinositide 3 kinase (PI3K) (Downward, 2004; Van Stry et al., 2005; Xiong et al., 2010). Additionally, PI3K is the major effector of Pdgfra regulating craniofacial development in mouse (Klinghoffer et al., 2002). In different *in vitro* analyses, ethanol has been suggested to downregulate several components of the PI3K pathway, including PI3K itself, AKT and mTOR, both downstream of PI3K (Guo et al., 2009; Hong-Brown et al., 2010; Vary et al., 2008; Xu et al., 2003). We hypothesized that PI3K signaling mediates Pdgfra protection from ethanol-induced apoptosis. We increased PI3K signaling by injecting untreated and ethanol-treated hypomorphic *pdgfra* mutants with morpholinos against the negative regulator of PI3K, *pten* (Croushore et al., 2005). These injections left wild-type and heterozygous embryos largely unaffected when compared with controls (supplementary material Figs S8, S9). Upregulating the PI3K pathway in either untreated or ethanol-treated mutants nearly fully rescued the palate defects when compared with untreated and ethanol-treated mutant controls (Fig. 5A-D). Injection of *pten* morpholinos also rescued the pharyngeal skeletal elements of ethanol-treated mutants to a nearly wild-type appearance (Fig. 5A′, compare with 5D′).

We wanted to test whether activation of this pathway at the level of mTOR could also rescue the ethanol-induced mutant phenotypes. L-Leucine has been shown to increase mTOR activity, leading to a rise in cell growth and survival (Hong-Brown et al., 2012; Kimball and Jefferson, 2006). Supplementing ethanol with 50 mM L-leucine partially rescued the ethanol-treated phenotype (Fig. 5E-F′), and had no apparent effect on either untreated heterozygote or wild-type silbings (supplementary material Fig. S10). However, a 10-24 hpf ethanol treatment with L-leucine treatment alone from 24 to 48 hpf did not rescue ethanol-induced defects in mutants (supplementary material Fig. S11, compare with Fig. 1). These data show that elevating either PI3K or mTOR signaling is sufficient to protect against ethanol-induced craniofacial defects in a Pdgfra attenuated embryo.

If the *pdgfra*/ethanol interaction is due to inhibition of the PI3K pathway downstream of Pdgfra, then pharmacological blockade of the PI3K pathway should recapitulate the ethanol defects in *pdgfra* mutants. Consistent with this model, treating *pdgfra* mutants with inhibitors of either PI3K (wortmannin) or mTOR (rapamycin) from 10 hpf to 24 hpf phenocopied the ethanol-induced defects of the palatal skeleton (Fig. 6F,I,L,M; supplementary material Fig. S12) and caused reductions in the pharyngeal skeleton compared with mutant controls and inhibitor-treated wild-type and heterozygous counterparts (Fig. 7F,I,L-O). Furthermore, these treatments also uncovered latent haploinsufficiency, causing variable defects, including those affecting the ethmoid plate and trabeculae (Fig. 6H,K,M). Although there are subtle differences between the treatments that could be due to dose or mechanism of action, the overall pattern of pharyngeal reduction is highly similar across treatments (Fig. 7). These data suggest that attenuation of the PI3K-mTOR pathway may underlie the *pdgfra*/ethanol interaction.

To directly test the effects of ethanol on the PI3K pathway in *pdgfra* mutants, we detected phosphorylated forms of the PI3K target AKT and the mTOR target eIF4B (Fig. 8). Heads from untreated and ethanol-treated *pdgfra* mutants and siblings were collected at 24 hpf. Downstream of mTOR, ethanol-treated mutants showed a decrease in levels of phospho-eIF4B compared with untreated embryos and ethanol-treated controls (Fig. 8C,D). Upstream of mTOR, we observed an increase in levels of phospho-AKT in both ethanol-treated mutants and controls compared with their untreated counterparts (Fig. 8A,B). These data are consistent with a growing body of evidence, primarily *in vitro* and in cancer models, that shows that inhibiting mTOR leads to an increase in AKT phosphorylation (Carracedo and Pandolfi, 2008; Hsu et al., 2011; Soares et al., 2013). To validate this feedback in the developing zebrafish, we assayed phospho-AKT levels in rapamycin-treated embryos. Indeed, blocking mTOR led to an increase in levels of phosphorylated AKT in both mutants and wild types compared with DMSO-treated controls (supplementary material Fig. S13), similar to the effects of ethanol. These data

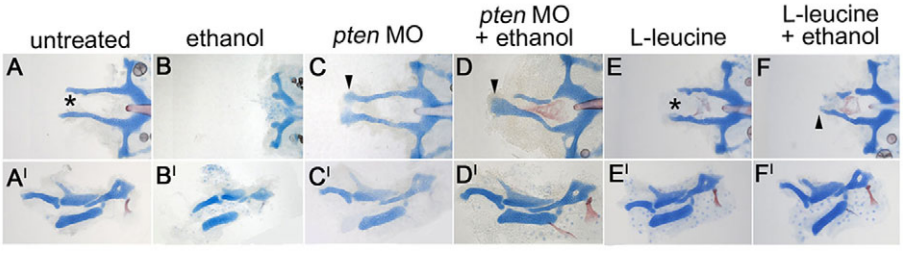

Fig. 5. Elevating PI3K/mTOR signaling rescues the craniofacial defects in ethanol-treated *pdgfra* mutants. (A-F′) 5 dpf *pdgfra* mutant neurocrania (A-F) and the corresponding pharyngeal skeletal elements (A′-F′). (**A**,**A′**) Untreated mutants have clefting of the ethmoid plate (asterisk, *n*=10/10). (**B**,**B′**) Treatment with 1.0% ethanol at 10-24 hpf causes loss of the palatal skeleton and hypoplasia of the pharyngeal skeleton (*n*=12/12). (**C-D′**) *pten* morpholino (MO) injection rescues the craniofacial phenotypes of both (C,C′, *n*=4/4) untreated and (D,D′, *n*=8/20) ethanol exposed *pdgfra* mutants. (**E**,**E′**) Most L-leucine-treated mutants have trabeculae (*n*=12/17; five embryos lacked trabeculae). (**F**,**F′**) Supplementing ethanol-treated mutants with L-leucine causes rescue of the trabeculae (*n*=10/32). Arrowheads mark the partially rescued ethmoid plates. Asterisk in E indicates clefting of the ethmoid plate.

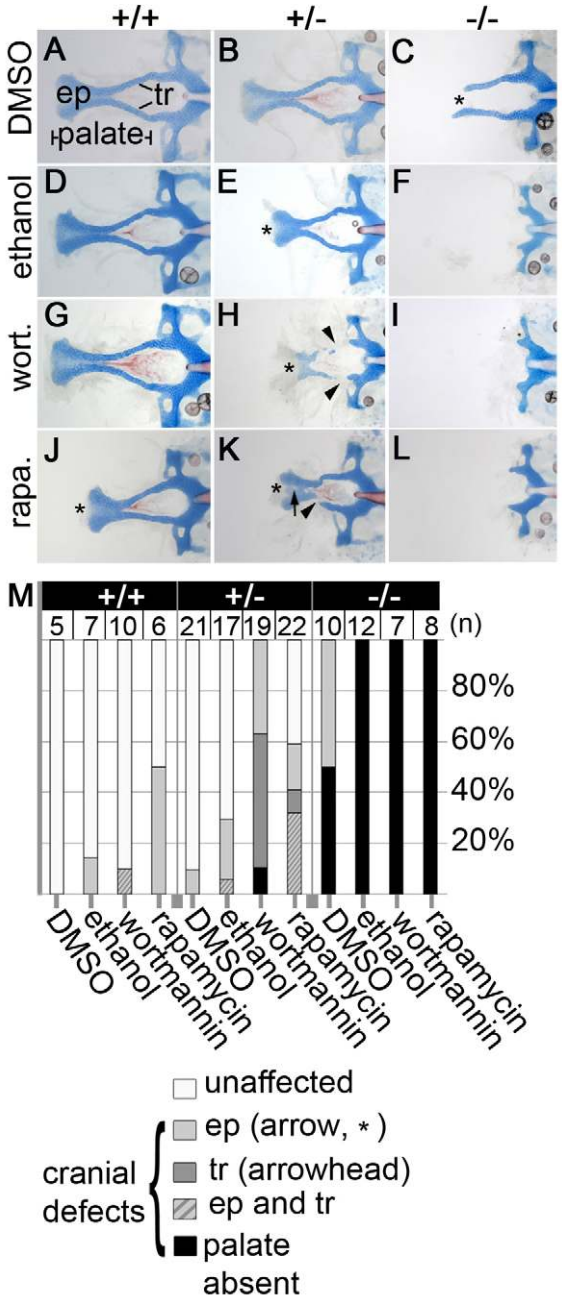

Fig. 6. Wortmannin and rapamycin phenocopy ethanol-treated *pdgfra* mutants. (**A-L**) 5 dpf zebrafish neurocrania embryos were treated at 10-24 hpf with (A-C) DMSO, (D-F) 1.0% ethanol, (G-I) 1.5 µM wortmannin or (J-L) 3 µM rapamycin. Asterisks indicate ethmoid-plate defects (ep); arrowheads indicate trabeculae defects (tr). (**M**) Graph of percentage defects found in all three genotypes, across treatments. Unaffected, wild-type phenotype; ep, ethmoid-plate defects (arrow and asterisk in K); tr, trabeculae defects (arrowheads in H).

support a model in which ethanol, in combination with loss of Pdgf signaling, attenuates the activity of mTOR, leading to hypophosphorylation of targets such as eIF4B, but also an increase in phosphorylated AKT.

DISCUSSION

Collectively, our results provide insight into the genetic susceptibility to ethanol-induced defects. Using zebrafish, we show that attenuated Pdgf signaling and ethanol exposure synergistically interact to cause variable craniofacial defects. This interaction may be conserved in humans, through our analysis of the human datatset herein, although further analysis in humans is necessary to confirm this finding. We suggest a model in which attenuated growth factor signaling interacts with ethanol to reduce the activity of PI3K/mTOR signaling, at or downstream of mTOR, thus causing developmental perturbations. At low levels of attenuation, whether from slight reduction in growth factor signaling or from low doses of ethanol, the system can compensate. However, those embryos with reduced growth factor signaling, even reductions that would not cause defects alone, that receive a ‘second hit’ via ethanol, can develop craniofacial defects.

pdgfra regulates both neural-crest cell migration and protection from ethanol-induced apoptosis

Pdgf signaling is essential for midfacial development across vertebrate species (Eberhart et al., 2008; Soriano, 1997; Tallquist and Soriano, 2003). At least in zebrafish, Pdgfra regulates the appropriate migration of neural-crest cells that will generate the midfacial skeleton (Eberhart et al., 2008). It is only in the presence of ethanol that we reveal the requirement of Pdgfra signaling in neural-crest cell survival. The increased apoptosis in ethanol-treated *pdgfra* mutants could be attributed to the fact that the *pdgra*$^{b1059/b1059}$ mutant allele is a hypomorph (Eberhart et al., 2008). In this model, the amount of Pdgfra signaling left in the hypomorph is sufficient for cellular survival. However, in the presence of ethanol, these signals no longer promote survival. This model is consistent with the finding that there is elevated cell death in *Pdgfra*-null mice (Soriano, 1997). However, in a neural crest conditional *Pdgfra* mutant, apoptosis did not appear elevated (Tallquist and Soriano, 2003), which may suggest an alternate model. The *pdgfra*-ethanol interaction could be due to broad inhibition of mTOR signaling, across growth factor pathways. The zebrafish mutation project (http://www.sanger.ac.uk/Projects/D_rerio/zmp/) has identified a putative null *pdgfra* allele. Analysis of this mutant allele will aid in distinguishing between these two possibilities.

Correct Pdgfra signaling relies heavily on PI3K activation. In mouse, knockout of the PI3K domain of *Pdgfra* leads to craniofacial defects, which mimic the full knockout phenotype (Klinghoffer et al., 2002). In frog, the PI3K domain of *Pdgfra* is necessary and sufficient for proper mesoderm migration and survival (Nagel et al., 2004; Van Stry et al., 2005). In our studies, increasing PI3K-mediated signaling through *pten* morpholino knockdown leads to a near wild-type phenotype in both untreated and ethanol-treated *pdgfra* mutants. This finding suggests that increasing PI3K function in ethanol-treated *pdgfra* mutant embryos rescues both survival and migration, as the midline defects are due to a migratory defect.

Although elevating PI3K signaling does rescue the defects in *pdgfra* mutants, understanding the precise mechanism will require additional studies. GTPases, which promote migration, and AKT, which supports survival and migration, rely on the PIP3 substrate of PI3K (Zhou and Huang, 2010). Thus, it is possible that the migratory and survival functions of Pdgfra are controlled by different signaling components immediately downstream of PI3K.

mTOR most likely regulates cell survival and growth in ethanol-treated embryos. L-leucine supplementation does not rescue the midline defects in our *pdgfra* mutants, which are caused by a migratory defect. In ethanol-treated mutants, we observe a decrease in the levels of activated eIF4B and an increase in levels of activated AKT, suggesting that ethanol impairs growth signaling at the level of mTOR or below. Further evidence that ethanol may be impairing

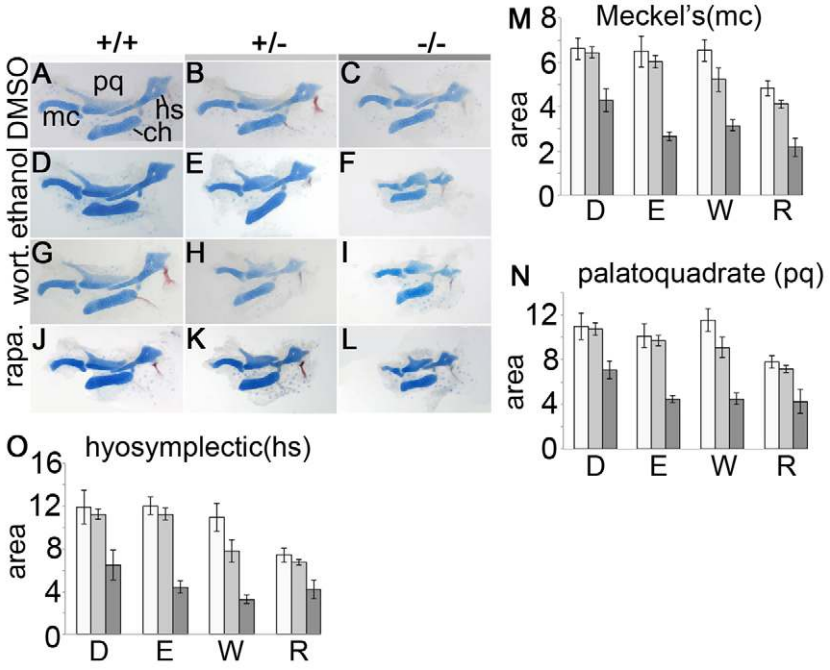

Fig. 7. Wortmannin or rapamycin induces pharyngeal skeleton hypoplasia in *pdgfra* mutants. (**A-L**) Embryos were treated at 10-24 hpf with (A-C) DMSO, (D-F) 1.0% ethanol, (G-I) 1.5 μM wortmannin or (J-L) 3 μM rapamycin. (**M-O**) Graphs depict the average area sizes, in thousands of μm^2 in (M) the Meckel's (mc), (N) palatoquadrate (pq) and (O) hyosymplectic (hs) cartilages. D, DMSO; E, ethanol; W, wortmannin, R, rapamycin [standard error bars are depicted at 1.5 s.e.m., significance is indicated by non-overlapping bars (Moses, 1987)]. Wild-type, light bar; *pdgfra* heterozygote, light-gray bar; mutant, dark-gray bar; ch, ceratohyal. Group numbers are the same as for Fig. 6.

mTOR activity specifically is the finding that phosphorylated levels of AKT are increased in ethanol treatment. A similar increase in activated AKT is observed in our model via rapamycin treatment of *pdgfra* mutants. Blocking mTOR function may release inhibitory feedback loops; for example, pancreatic cancer cells treated with rapamycin show elevated levels of phosphorylated AKT compared with untreated controls (Soares et al., 2013). It is interesting to speculate that the upregulation of AKT in ethanol-treated siblings may buffer against deleterious phenotypes by elevating cell proliferation. However, a more extensive analysis of the PI3K and mTOR pathways will be necessary to fully understand how Pdgfra-mediated migration and protection are controlled intracellularly.

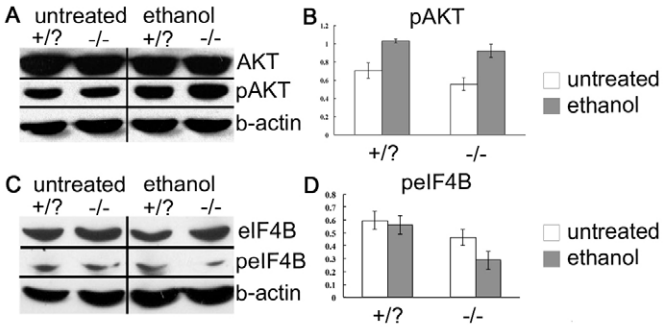

Fig. 8. Ethanol alters phosphorylation of AKT and pEIF4B in *pdgfra* mutants. Heads of 24 hpf *pdgfra* mutant (–/–) and *pdgfra* sibling (+/?) from untreated controls or embryos treated with 1.0% ethanol from 10-24 hpf were used. (**A**) Immunoblot was stripped and reprobed for total AKT, phospho-AKT (pAKT) and β-actin as a loading control. Both ethanol-treated *pdgfra* siblings and *pdgfra* mutants have elevated levels of phospho-AKT compared with untreated counterparts. (**B**) Ratio of pAKT to total AKT across three immunoblots. (**C**) Immunoblot was stripped and reprobed for total eIF4B (eIF4B), phospho-eIF4B (peIF4B) and β-actin as a loading control. *pdgfra* mutants have decreased levels of phospho-eIF4B compared with untreated mutants, and both untreated and ethanol-treated siblings samples. (**D**) Ratio of phospho-eIF4B to total eIF4B across three immunoblots.

Ethanol may broadly disrupt growth-factor signaling pathways

The interaction observed between ethanol and *pdgfra* supports a model in which PI3K-dependent growth factor genes interact with ethanol. Notable among these genes is *insulin receptor* (*insr*). Insr functions in proper brain development. Reducing the expression of *Insr* in newly born rat pups causes defects similar to those found in rat models of FASD (de la Monte et al., 2011). Increasing insulin receptor expression in a *Drosophila* model of FASD rescues neurobehavioral defects caused by ethanol exposure (McClure et al., 2011). These data, along with our observations of *pdgfra*, strongly suggest that growth factor genes play a significant role in the susceptibility to ethanol teratogenesis. Because growth factor signaling is used throughout development, attenuated growth factor signaling, along with ethanol exposure, could explain a large part of the variability found in FASD. This model is consistent with the human dataset in which the phenotypes associated with gene/ethanol interactions are different between *PDGFRA* and *PDGFRB*. As the human dataset grows, it will be of great interest to examine further the extent of interactions between ethanol and PI3K-dependent growth factors.

Zebrafish as a model of gene-environment interactions

The zebrafish provides a powerful tool in uncovering both the genetics and the mechanisms of FASD susceptibility. Owing to the array of genetic resources available and the ease of administering ethanol to the externally fertilized embryos, it is feasible to screen hundreds of genes rapidly. As we have done here, findings in zebrafish can be used to direct analyses in human datasets that may not yet be large enough for genome-wide power. Although the human dataset we analyzed is small, by focusing on a small number of genes, the likelihood of detecting false associations was greatly decreased. After correcting for the testing of SNPs across five genes, and therefore five essentially independent tests, the associations we found in the genes encoding for the human PDGF receptors were significant, with $P<0.01$. This significant association even

withstands a more strict correction of treating all 118 SNPs as independent tests ($0.05/118=4.2\times10^{-4}$). Thus, the zebrafish model guided focused studies in a human dataset and allowed us to detect a gene-ethanol interaction contributing to the variation in craniofacial measures. Importantly, owing to the conservation of gene function across vertebrate species, we can understand the mechanism of these interactions using the zebrafish model system. Collectively, our findings provide a predictive mechanistic model for some gene-ethanol interactions that underlie the craniofacial defects in FASD.

Although we have focused on the craniofacial aspect of FASD, the zebrafish provides an excellent model in which to study the neural aspects of FASD. The brain is the most commonly affected organ in FASD, with defects to the cerebellum and oligodendrocytes being common (Hoyme et al., 2005; Swayze et al., 1997). *Pdgfra* is important for oligodendrocyte maturation and migration in mouse (McKinnon et al., 2005), although the function of *pdgfra* in zebrafish oligodendrocyte development has not been tested. It would be of interest to determine if oligodendrocytes are disrupted in ethanol-treated *pdgfra* mutants.

Owing to its genetic tractability the zebrafish has long been a valuable model system for understanding developmental processes. We currently understand an enormous amount regarding the genetics regulating development from work in numerous model systems. Due to the level of this understanding, we are now well poised to gain substantial knowledge about how the environment impinges on the genetic networks underlying development (so called Eco-Devo). Our work here and recent work examining gene-environment interactions underlying ototoxicity (Coffin et al., 2010) demonstrate that the same characteristics (e.g. genetic amenability, ease of imaging and external fertilization) that make zebrafish useful for understanding development make it useful for understanding Eco-Devo.

Acknowledgements
We thank Jeffrey Gross for help on the western blot analysis and Jennifer Morgan, for use of her lab's analytical software. For the GC analysis, we thank both Rueben Gonzalez and Regina Nobles. We would also thank Michael Charness and Ed Riley for their advice and input in the preparation of this manuscript, and Young-Jun Jeon for his advice regarding ethanol and mTOR.

Funding
Funding to support this research was provided by the National Institutes of Health/National Institute of Dental and Craniofacial Research (NIH/NIDCR) [R01DE020884]; by grants from the The Foundation for Alcohol Research (ABMRF) to J.K.E. and from the NIH/National Institute on Alcohol Abuse and Alcoholism (NIAAA) [U01AA014809 10 to T.M.F.]; by a Bruce/Jones Fellowship and a NIH/NIAAA grant [F31AA020731 to N.M.]; and by a NIH/NIAAA grant [F32AA021320 to C.B.L.]. We also thank Charles B. Kimmel and the University of Oregon Fish researchers and staff for their contributions to the forward genetic screen [P01 HD22486 to C. B. Kimmel]. Deposited in PMC for immediate release.

Competing interests statement
The authors declare no competing financial interests.

Author contributions
N.M. and J.K.E. conceived, wrote and edited the manuscript. N.M. performed all of the characterizations of the *pdgfra*/ethanol interaction in zebrafish. L.W. and T.M.F. performed and analyzed the human data and edited the manuscript. M.E.S. assisted with the initial discovery of the *pdgfra*/ethanol interaction, performed the miR140 morpholino and *in situ* hybridization experiments and edited the manuscript. C.B.L. determined the tissue levels of ethanol in treated embryos and edited the manuscript.

Supplementary material
Supplementary material available online at
http://dev.biologists.org/lookup/suppl/doi:10.1242/dev.094938/-/DC1

References

Ali, S., Champagne, D. L., Alia, A. and Richardson, M. K. (2011). Large-scale analysis of acute ethanol exposure in zebrafish development: a critical time window and resilience. *PLoS ONE* **6**, e20037.
Arenzana, F. J., Carvan, M. J., 3rd, Aijón, J., Sánchez-González, R., Arévalo, R. and Porteros, A. (2006). Teratogenic effects of ethanol exposure on zebrafish visual system development. *Neurotoxicol. Teratol.* **28**, 342-348.
Boehm, S. L., II, Lundahl, K. R., Caldwell, J. and Gilliam, D. M. (1997). Ethanol teratogenesis in the C57BL/6J, DBA/2J, and A/J inbred mouse strains. *Alcohol* **14**, 389-395.
Carracedo, A. and Pandolfi, P. P. (2008). The PTEN-PI3K pathway: of feedbacks and cross-talks. *Oncogene* **27**, 5527-5541.
Cartwright, M. M. and Smith, S. M. (1995). Stage-dependent effects of ethanol on cranial neural crest cell development: partial basis for the phenotypic variations observed in fetal alcohol syndrome. *Alcohol. Clin. Exp. Res.* **19**, 1454-1462.
Coffin, A. B., Ou, H., Owens, K. N., Santos, F., Simon, J. A., Rubel, E. W. and Raible, D. W. (2010). Chemical screening for hair cell loss and protection in the zebrafish lateral line. *Zebrafish* **7**, 3-11.
Couly, G. F., Coltey, P. M. and Le Douarin, N. M. (1993). The triple origin of skull in higher vertebrates: a study in quail-chick chimeras. *Development* **117**, 409-429.
Croushore, J. A., Blasiole, B., Riddle, R. C., Thisse, C., Thisse, B., Canfield, V. A., Robertson, G. P., Cheng, K. C. and Levenson, R. (2005). Ptena and ptenb genes play distinct roles in zebrafish embryogenesis. *Dev. Dyn.* **234**, 911-921.
Crump, J. G., Maves, L., Lawson, N. D., Weinstein, B. M. and Kimmel, C. B. (2004). An essential role for Fgfs in endodermal pouch formation influences later craniofacial skeletal patterning. *Development* **131**, 5703-5716.
Crump, J. G., Swartz, M. E., Eberhart, J. K. and Kimmel, C. B. (2006). Moz-dependent Hox expression controls segment-specific fate maps of skeletal precursors in the face. *Development* **133**, 2661-2669.
Cubbage, C. C. and Mabee, P. M. (1996). Development of the cranium and paired fins in the zebrafish Danio rerio (Ostariophysi, Cyprinidae). *J. Morphol.* **229**, 121-160.
de la Monte, S. M., Tong, M., Bowling, N. and Moskal, P. (2011). si-RNA inhibition of brain insulin or insulin-like growth factor receptors causes developmental cerebellar abnormalities: relevance to fetal alcohol spectrum disorder. *Mol. Brain* **4**, 13.
Debelak, K. A. and Smith, S. M. (2000). Avian genetic background modulates the neural crest apoptosis induced by ethanol exposure. *Alcohol. Clin. Exp. Res.* **24**, 307-314.
Dlugos, C. A. and Rabin, R. A. (2003). Ethanol effects on three strains of zebrafish: model system for genetic investigations. *Pharmacol. Biochem. Behav.* **74**, 471-480.
Dougherty, M., Kamel, G., Grimaldi, M., Gfrerer, L., Shubinets, V., Ethier, R., Hickey, G., Cornell, R. A. and Liao, E. C. (2013). Distinct requirements for wnt9a and irf6 in extension and integration mechanisms during zebrafish palate morphogenesis. *Development* **140**, 76-81.
Downward, J. (2004). PI 3-kinase, Akt and cell survival. *Semin. Cell Dev. Biol.* **15**, 177-182.
Eberhart, J. K., Swartz, M. E., Crump, J. G. and Kimmel, C. B. (2006). Early Hedgehog signaling from neural to oral epithelium organizes anterior craniofacial development. *Development* **133**, 1069-1077.
Eberhart, J. K., He, X., Swartz, M. E., Yan, Y.-L., Song, H., Boling, T. C., Kunerth, A. K., Walker, M. B., Kimmel, C. B. and Postlethwait, J. H. (2008). MicroRNA Mirn140 modulates Pdgf signaling during palatogenesis. *Nat. Genet.* **40**, 290-298.
Evans, D. J. and Noden, D. M. (2006). Spatial relations between avian craniofacial neural crest and paraxial mesoderm cells. *Dev. Dyn.* **235**, 1310-1325.
Grevellec, A. and Tucker, A. S. (2010). The pharyngeal pouches and clefts: Development, evolution, structure and derivatives. *Semin. Cell Dev. Biol.* **21**, 325-332.
Gross, J. B. and Hanken, J. (2008). Review of fate-mapping studies of osteogenic cranial neural crest in vertebrates. *Dev. Biol.* **317**, 389-400.
Guo, R., Zhong, L. and Ren, J. (2009). Overexpression of aldehyde dehydrogenase-2 attenuates chronic alcohol exposure-induced apoptosis, change in Akt and Pim signalling in liver. *Clin. Exp. Pharmacol. Physiol.* **36**, 463-468.
Hong, M. and Krauss, R. S. (2012). Cdon mutation and fetal ethanol exposure synergize to produce midline signaling defects and holoprosencephaly spectrum disorders in mice. *PLoS Genet.* **8**, e1002999.
Hong-Brown, L. Q., Brown, C. R., Kazi, A. A., Huber, D. S., Pruznak, A. M. and Lang, C. H. (2010). Alcohol and PRAS40 knockdown decrease mTOR activity and protein synthesis via AMPK signaling and changes in mTORC1 interaction. *J. Cell. Biochem.* **109**, 1172-1184.
Hong-Brown, L. Q., Brown, C. R., Kazi, A. A., Navaratnarajah, M. and Lang, C. H. (2012). Rag GTPases and AMPK/TSC2/Rheb mediate the differential

regulation of mTORC1 signaling in response to alcohol and leucine. *Am. J. Physiol.* **302**, C1557-C1565.
Hoyme, H. E., May, P. A., Kalberg, W. O., Kodituwakku, P., Gossage, J. P., Trujillo, P. M., Buckley, D. G., Miller, J. H., Aragon, A. S., Khaole, N. et al. (2005). A practical clinical approach to diagnosis of fetal alcohol spectrum disorders: clarification of the 1996 institute of medicine criteria. *Pediatrics* **115**, 39-47.
Hsu, P. P., Kang, S. A., Rameseder, J., Zhang, Y., Ottina, K. A., Lim, D., Peterson, T. R., Choi, Y., Gray, N. S., Yaffe, M. B. et al. (2011). The mTOR-regulated phosphoproteome reveals a mechanism of mTORC1-mediated inhibition of growth factor signaling. *Science* **332**, 1317-1322.
Jones, K. L. and Smith, D. W. (1973). Recognition of the fetal alcohol syndrome in early infancy. *Lancet* **302**, 999-1001.
Jones, K. L., Robinson, L. K., Bakhireva, L. N., Marintcheva, G., Storojev, V., Strahova, A., Sergeevskaya, S., Budantseva, S., Mattson, S. N., Riley, E. P. et al. (2006). Accuracy of the diagnosis of physical features of fetal alcohol syndrome by pediatricians after specialized training. *Pediatrics* **118**, e1734-8.
Kesteven, H. L. (1922). A new interpretation of the bones in the palate and upper jaw of fishes: Part I. *J. Anat.* **56**, 307-324.
Kimball, S. R. and Jefferson, L. S. (2006). Signaling pathways and molecular mechanisms through which branched-chain amino acids mediate translational control of protein synthesis. *J. Nutr.* **136 Suppl.**, 227S-231S.
Kimmel, C. B., Miller, C. T., Kruze, G., Ullmann, B., BreMiller, R. A., Larison, K. D. and Snyder, H. C. (1998). The shaping of pharyngeal cartilages during early development of the zebrafish. *Dev. Biol.* **203**, 245-263.
Klinghoffer, R. A., Hamilton, T. G., Hoch, R. and Soriano, P. (2002). An allelic series at the PDGFalphaR locus indicates unequal contributions of distinct signaling pathways during development. *Dev. Cell* **2**, 103-113.
Knight, R. D. and Schilling, T. F. (2006). Cranial neural crest and development of the head skeleton. *Adv. Exp. Med. Biol.* **589**, 120-133.
Lange, J. E. and Voas, R. B. (2000). Defining binge drinking quantities through resulting BACs. *Annu. Proc. Assoc. Adv. Automot. Med.* **44**, 389-404.
Lawson, N. D. and Weinstein, B. M. (2002). In vivo imaging of embryonic vascular development using transgenic zebrafish. *Dev. Biol.* **248**, 307-318.
Le Lièvre, C. S. (1978). Participation of neural crest-derived cells in the genesis of the skull in birds. *J. Embryol. Exp. Morphol.* **47**, 17-37.
Lockwood, B., Bjerke, S., Kobayashi, K. and Guo, S. (2004). Acute effects of alcohol on larval zebrafish: a genetic system for large-scale screening. *Pharmacol. Biochem. Behav.* **77**, 647-654.
Loucks, E. and Carvan, M. J., III (2004). Strain-dependent effects of developmental ethanol exposure in zebrafish. *Neurotoxicol. Teratol.* **26**, 745-755.
Mattson, S. N., Foroud, T., Sowell, E. R., Jones, K. L., Coles, C. D., Fagerlund, A., Autti-Rämö, I., May, P. A., Adnams, C. M., Konovalova, V. et al.; CIFASD (2010). Collaborative initiative on fetal alcohol spectrum disorders: methodology of clinical projects. *Alcohol* **44**, 635-641.
Maves, L., Jackman, W. and Kimmel, C. B. (2002). FGF3 and FGF8 mediate a rhombomere 4 signaling activity in the zebrafish hindbrain. *Development* **129**, 3825-3837.
May, P. A., Gossage, J. P., Brooke, L. E., Snell, C. L., Marais, A. S., Hendricks, L. S., Croxford, J. A. and Viljoen, D. L. (2005). Maternal risk factors for fetal alcohol syndrome in the Western cape province of South Africa: a population-based study. *Am. J. Public Health* **95**, 1190-1199.
May, P. A., Gossage, J. P., Marais, A. S., Adnams, C. M., Hoyme, H. E., Jones, K. L., Robinson, L. K., Khaole, N. C., Snell, C., Kalberg, W. O. et al. (2007). The epidemiology of fetal alcohol syndrome and partial FAS in a South African community. *Drug Alcohol Depend.* **88**, 259-271.
McClure, K. D., French, R. L. and Heberlein, U. (2011). A Drosophila model for fetal alcohol syndrome disorders: role for the insulin pathway. *Dis. Model. Mech.* **4**, 335-346.
McKinnon, R. D., Waldron, S. and Kiel, M. E. (2005). PDGF alpha-receptor signal strength controls an RTK rheostat that integrates phosphoinositol 3′-kinase and phospholipase Cgamma pathways during oligodendrocyte maturation. *J. Neurosci.* **25**, 3499-3508.
Moore, E. S., Ward, R. E., Wetherill, L. F., Rogers, J. L., Autti-Rämö, I., Fagerlund, A., Jacobson, S. W., Robinson, L. K., Hoyme, H. E., Mattson, S. N. et al.; CIFASD (2007). Unique facial features distinguish fetal alcohol syndrome patients and controls in diverse ethnic populations. *Alcohol. Clin. Exp. Res.* **31**, 1707-1713.
Moses, L. E. (1987). Graphical methods in statistical analysis. *Annu. Rev. Public Health* **8**, 309-353.
Nagel, M., Tahinci, E., Symes, K. and Winklbauer, R. (2004). Guidance of mesoderm cell migration in the Xenopus gastrula requires PDGF signaling. *Development* **131**, 2727-2736.
Noden, D. M. (1978). The control of avian cephalic neural crest cytodifferentiation. I. Skeletal and connective tissues. *Dev. Biol.* **67**, 296-312.
Payne, E. M., Virgilio, M., Narla, A., Sun, H., Levine, M., Paw, B. H., Berliner, N., Look, A. T., Ebert, B. L. and Khanna-Gupta, A. (2012). L-Leucine improves the anemia and developmental defects associated with Diamond-Blackfan anemia and del(5q) MDS by activating the mTOR pathway. *Blood* **120**, 2214-2224.
Price, A. L., Patterson, N. J., Plenge, R. M., Weinblatt, M. E., Shadick, N. A. and Reich, D. (2006). Principal components analysis corrects for stratification in genome-wide association studies. *Nat. Genet.* **38**, 904-909.
Sampson, P. D., Streissguth, A. P., Bookstein, F. L., Little, R. E., Clarren, S. K., Dehaene, P., Hanson, J. W. and Graham, J. M., Jr (1997). Incidence of fetal alcohol syndrome and prevalence of alcohol-related neurodevelopmental disorder. *Teratology* **56**, 317-326.
Schneider, C. A., Rasband, W. S. and Eliceiri, K. W. (2012). NIH Image to ImageJ: 25 years of image analysis. *Nat. Methods* **9**, 671-675.
Shah, R. M., Donaldson, E. M. and Scudder, G. G. (1990). Toward the origin of the secondary palate. A possible homologue in the embryo of fish, Onchorhynchus kisutch, with description of changes in the basement membrane area. *Am. J. Anat.* **189**, 329-338.
Sheehan-Rooney, K., Swartz, M. E., Lovely, C. B., Dixon, M. J. and Eberhart, J. K. (2013). Bmp and Shh signaling mediate the expression of satb2 in the pharyngeal arches. *PLoS ONE* **8**, e59533.
Soares, H. P., Ni, Y., Kisfalvi, K., Sinnett-Smith, J. and Rozengurt, E. (2013). Different patterns of Akt and ERK feedback activation in response to rapamycin, active-site mTOR inhibitors and metformin in pancreatic cancer cells. *PLoS ONE* **8**, e57289.
Soriano, P. (1997). The PDGF alpha receptor is required for neural crest cell development and for normal patterning of the somites. *Development* **124**, 2691-2700.
Stockard, C. (1910). The influence of alcohol and other anaesthetics on embryonic development. *Am. J. Anat.* **10**, 369-392.
Streissguth, A. P. and Dehaene, P. (1993). Fetal alcohol syndrome in twins of alcoholic mothers: concordance of diagnosis and IQ. *Am. J. Med. Genet.* **47**, 857-861.
Sulik, K. K. (2005). Genesis of alcohol-induced craniofacial dysmorphism. *Exp. Biol. Med. (Maywood)* **230**, 366-375.
Sulik, K. K., Johnston, M. C., Daft, P. A., Russell, W. E. and Dehart, D. B. (1986). Fetal alcohol syndrome and DiGeorge anomaly: critical ethanol exposure periods for craniofacial malformations as illustrated in an animal model. *Am. J. Med. Genet. Suppl.* **2**, 97-112.
Swartz, M. E., Sheehan-Rooney, K., Dixon, M. J. and Eberhart, J. K. (2011). Examination of a palatogenic gene program in zebrafish. *Dev. Dyn.* **240**, 2204-2220.
Swayze, V. W., II, Johnson, V. P., Hanson, J. W., Piven, J., Sato, Y., Giedd, J. N., Mosnik, D. and Andreasen, N. C. (1997). Magnetic resonance imaging of brain anomalies in fetal alcohol syndrome. *Pediatrics* **99**, 232-240.
Tallquist, M. and Kazlauskas, A. (2004). PDGF signaling in cells and mice. *Cytokine Growth Factor Rev.* **15**, 205-213.
Tallquist, M. D. and Soriano, P. (2003). Cell autonomous requirement for PDGFRalpha in populations of cranial and cardiac neural crest cells. *Development* **130**, 507-518.
Theveneau, E. and Mayor, R. (2012). Neural crest delamination and migration: from epithelium-to-mesenchyme transition to collective cell migration. *Dev. Biol.* **366**, 34-54.
Thomas, J. D., Melcer, T., Weinert, S. and Riley, E. P. (1998). Neonatal alcohol exposure produces hyperactivity in high-alcohol-sensitive but not in low-alcohol-sensitive rats. *Alcohol* **16**, 237-242.
Tittle, R. K., Sze, R., Ng, A., Nuckels, R. J., Swartz, M. E., Anderson, R. M., Bosch, J., Stainier, D. Y., Eberhart, J. K. and Gross, J. M. (2011). Uhrf1 and Dnmt1 are required for development and maintenance of the zebrafish lens. *Dev. Biol.* **350**, 50-63.
Van Stry, M., McLaughlin, K. A., Ataliotis, P. and Symes, K. (2004). The mitochondrial-apoptotic pathway is triggered in Xenopus mesoderm cells deprived of PDGF receptor signaling during gastrulation. *Dev. Biol.* **268**, 232-242.
Van Stry, M., Kazlauskas, A., Schreiber, S. L. and Symes, K. (2005). Distinct effectors of platelet-derived growth factor receptor-alpha signaling are required for cell survival during embryogenesis. *Proc. Natl. Acad. Sci. USA* **102**, 8233-8238.
Varga, Z. M., Amores, A., Lewis, K. E., Yan, Y. L., Postlethwait, J. H., Eisen, J. S. and Westerfield, M. (2001). Zebrafish smoothened functions in ventral neural tube specification and axon tract formation. *Development* **128**, 3497-3509.
Vary, T. C., Deiter, G. and Lantry, R. (2008). Chronic alcohol feeding impairs mTOR(Ser 2448) phosphorylation in rat hearts. *Alcohol. Clin. Exp. Res.* **32**, 43-51.
Viljoen, D. L., Carr, L. G., Foroud, T. M., Brooke, L., Ramsay, M. and Li, T. K. (2001). Alcohol dehydrogenase-2*2 allele is associated with decreased prevalence of fetal alcohol syndrome in the mixed-ancestry population of the Western Cape Province, South Africa. *Alcohol. Clin. Exp. Res.* **25**, 1719-1722.
Walker, M. B. and Kimmel, C. B. (2007). A two-color acid-free cartilage and bone stain for zebrafish larvae. *Biotech. Histochem.* **82**, 23-28.
Warren, K. R. and Li, T. K. (2005). Genetic polymorphisms: impact on the risk of fetal alcohol spectrum disorders. *Birth Defects Res. A Clin. Mol. Teratol.* **73**, 195-203.
Westerfield, M. (1993). *The Zebrafish Book: A Guide For the Laboratory Use of Zebrafish (Brachydanio Rerio)*. Eugene, OR: University of Oregon Press.

Wu, E., Palmer, N., Tian, Z., Moseman, A. P., Galdzicki, M., Wang, X., Berger, B., Zhang, H. and Kohane, I. S. (2008). Comprehensive dissection of PDGF-PDGFR signaling pathways in PDGFR genetically defined cells. *PLoS ONE* **3**, e3794.

Xiong, W., Cheng, B. H., Jia, S. B. and Tang, L. S. (2010). Involvement of the PI3K/Akt signaling pathway in platelet-derived growth factor-induced migration of human lens epithelial cells. *Curr. Eye Res.* **35**, 389-401.

Xu, J., Yeon, J. E., Chang, H., Tison, G., Chen, G. J., Wands, J. and de la Monte, S. (2003). Ethanol impairs insulin-stimulated neuronal survival in the developing brain: role of PTEN phosphatase. *J. Biol. Chem.* **278**, 26929-26937.

Yoshida, T., Vivatbutsiri, P., Morriss-Kay, G., Saga, Y. and Iseki, S. (2008). Cell lineage in mammalian craniofacial mesenchyme. *Mech. Dev.* **125**, 797-808.

Zhang, C., Ojiaku, P. and Cole, G. J. (2013). Forebrain and hindbrain development in zebrafish is sensitive to ethanol exposure involving agrin, Fgf, and sonic hedgehog function. *Birth Defects Res. A Clin. Mol. Teratol.* **97**, 8-27.

Zhou, H. and Huang, S. (2010). The complexes of mammalian target of rapamycin. *Curr. Protein Pept. Sci.* **11**, 409-424.